

Miscibility and interactions in poly(*n*-propyl methacrylate)/poly(vinyl alcohol) blends

J.Z. Yi^{a,*}, S.H. Goh^b

^a*School of Chemistry and Chemical Engineering, Sun Yat-Sun University, Guangzhou 510275, People's Republic of China*

^b*Department of Chemistry, National University of Singapore, 3 Science Drive 3, Singapore 117543, Singapore*

Received 13 January 2005; received in revised form 31 May 2005; accepted 6 July 2005

Available online 19 August 2005

Abstract

Poly(*n*-propyl methacrylate) (PPMA) is miscible with poly(vinyl alcohol) (PVA) over the whole composition range as shown by the existence of a single glass transition temperature in each blend. The interaction between PPMA and PVA was examined by Fourier transform infrared spectroscopy and solid-state nuclear magnetic resonance spectroscopy. The interactions mainly involve the hydroxyl groups of PVA and the carbonyl groups of PPMA. The measurements of proton spin–lattice relaxation time reveal that PPMA and PVA do not mix intimately on a scale of 1–3 nm, but are miscible on a scale of 20–30 nm. A small negative interaction parameter value has been obtained by melting point depression measurement.

© 2005 Elsevier Ltd. All rights reserved.

Keywords: Blends; Miscibility; Glass transition temperature

1. Introduction

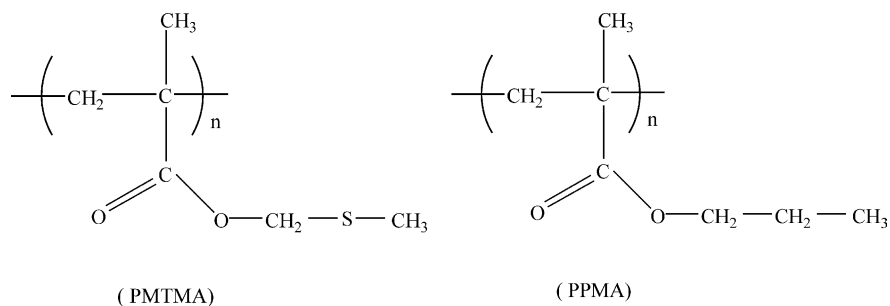
Hydroxyl-containing polymers are capable of forming miscible blends with proton-accepting polymers through hydrogen-bonding interactions through their hydroxyl groups [1]. However, hydroxyl-containing polymers are self-associated and hence the competition between self-association and interpolymer interaction plays an important role in determining the miscibility behavior of their blends. For example, poly(vinyl alcohol) (PVA) is miscible with three tertiary amide polymers poly(*N*-vinyl-2-pyrrolidone) (PVP) [2–6], poly(*N,N*-dimethylacrylamide) [7] and poly(2-methyl-2-oxazoline) [8], but is immiscible with another tertiary amide polymer poly(2-ethyl-2-oxazoline) (PEOx) [9]. PVA is miscible with hydroxyl-containing polymers such as poly(acrylic acid) (PAA) [10,11], poly(methacrylic

acid) [10], and cellulose [12]. The miscibility of PVA/chitin [13], PVA/poly(L-lactide) (PLLA) [14] and poly(vinyl acetate-*co*-vinyl alcohol)/PLLA [15] blends has been reported recently.

We have recently reported that both PVA and poly(*p*-vinylphenol) (PVPh) are miscible with poly(methylthio-methyl methacrylate) (PMTMA), mainly arising from interactions between the hydroxyl groups of PVA or PVPh and the thioether sulfur atoms of PMTMA [16,17]. Interactions involving the carbonyl groups of PMTMA are not significant [16,17]. We suggested that the big sulfur atom in the pendant group of PMTMA might have reduced the accessibility of the carbonyl groups. For comparison, we have studied the miscibility and interactions in blends of PVA with poly(*n*-propyl methacrylate) (PPMA), which does not contain sulfur atom in the pendant group. It will be shown that PVA is miscible with PPMA, arising from interactions between the hydroxyl groups of PVA and the carbonyl groups of PPMA. A small negative interaction parameter value has been obtained by melting point depression measurement.

* Corresponding author. Tel.: +86 20 841 40273.

E-mail address: cesyzj@zsu.edu.cn (J.Z. Yi).



2. Experimental section

2.1. Materials

PVA (weight-average molecular weight (M_w)=14,000) and PPMA (M_w =175,000) were supplied by BDH Chemical Ltd and Scientific Polymer Products, Inc., respectively.

2.2. Preparation of blends

PPMA and PVA were separately dissolved in dimethylformamide (DMF) to form 1% (w/v) solutions. Appropriate amounts of PPMA and PVA solutions were mixed under continuous stirring for 3 h. The solution was then allowed to evaporate to dryness to give a polymer blend. The blend was dried in vacuo at 60 °C for 2 weeks.

2.3. Glass-transition temperature measurements

The glass transition temperature (T_g) values of various blends were measured with a TA Instruments 2920 differential scanning calorimeter using a heating rate of 20 and 5 °C/min. Each sample was subjected to several heating/cooling cycles to obtain reproducible T_g values. The initial onset of the change of slope in the DSC curve is taken to be the T_g .

2.4. Fourier transform infrared spectroscopic characterization

FTIR spectra were acquired using a Bio-Rad 165 FTIR spectrophotometer. Samples were prepared by grinding the blends with KBr and compressing the mixture to form disks. The disks were stored in a desiccator to avoid moisture absorption. All spectra were recorded at 140 °C to ensure the exclusion of absorbed moisture. Sixteen scans were signal-averaged at a resolution of 4 cm^{-1} .

2.5. Nuclear magnetic resonance measurements

High-resolution solid-state ^{13}C NMR experiments were carried out on a Bruker DRX-400 MHz NMR spectrometer operating at resonance frequencies of 400 and 100 MHz for

^1H and ^{13}C , respectively. The high-resolution solid-state ^{13}C NMR spectra were obtained by using the cross polarization (CP)/magic angle spinning (MAS)/high-power dipolar decoupling (DD) technique. A 90° pulse width of 2.75 μs and a contact time of 3 ms were used in ^{13}C CP/MAS experiments. The MAS rate was 8 kHz for measurements of both ^{13}C spectra and relaxation time. The ^{13}C chemical shift of the methine carbon of solid adamantane (29.5 ppm relative to TMS) was used as an external reference standard.

3. Results and discussion

3.1. General characteristics of blends

All the DMF-cast PPMA/PVA blends were transparent and each showed a single T_g , indicating miscibility. As shown in Fig. 1, the T_g values of the PPMA/PVA blends are slightly lower than those predicted by the linear additivity rule. In comparison, the T_g values of the PMTMA/PVA blends are significantly larger than those predicted by the linear additivity rule [17]. The T_g -composition curves for PPMA/PVA and PMTMA/PVA blends can be fitted by the Kwei equation [18,19]:

$$T_g(\text{blend}) = \left[\frac{w_1 T_{g1} + k w_2 T_{g2}}{w_1 + k w_2} \right] + q w_1 w_2$$

where k and q are fitting constants. The curve in Fig. 1 was

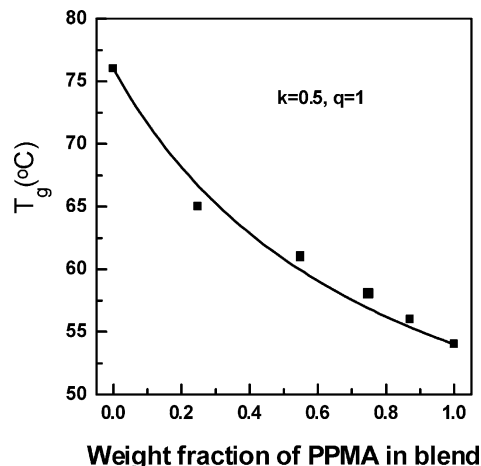


Fig. 1. T_g -composition curve of PPMA/PVA blends.

Table 1
Characteristics of PPMA/PVA blends

Blend	1	2	3	4
Feed composition ^a	0.25	0.55	0.75	0.97
Feed composition ^b	0.10	0.30	0.50	0.70
T_g (°C)	65	61	58	56
T_m (°C)	223	221	219	218
ΔH_f (J/g)	41.7	22.8	12.5	5.9
χ_c (%)	35.3	32.8	31.2	29.5

^a Weight fraction of PPMA.

^b Mole fraction of PPMA.

drawn using $k=0.5$ and $q=1$. The k and q values for PMTMA/PVA blends are 1 and 60 [17], respectively. The q value is commonly taken as a measurement of number of specific interactions [19]. Therefore, the smaller q value for the PPMA/PVA blends appears to suggest the existence of a smaller number of interactions in the PPMA/PVA blends than in the PMTMA/PVA blends. Table 1 lists the thermal characteristics of PPMA/PVA blends. The degree of the crystallinity of PVA is calculated by the following equation:

$$\chi_c = \frac{\Delta H_f}{\Delta H_w^0}$$

where ΔH_f is the apparent enthalpy of the fusion of PVA in the blend, W is the weight fraction of PVA, and ΔH_f^0 is the enthalpy of fusion of completely crystalline PVA (156 J/g for PVA [20]). For polymer blends containing a crystalline component, the variation in values of T_m and χ_c is usually attributed to interactions between the components [21–23]. The T_m and χ_c values decrease with increasing PPMA content in the blend, indicating the presence of interaction between PVA and PPMA. However, the suppression of the crystallization of PVA in the PPMA/PVA blends is not as severe as in the PMTMA/PVA blends. The crystallization of PVA is completely suppressed when the PMTMA content in the PMTMA/PVA blends reaches 50 mol% (or 30 wt%)

[17]. Similarly, the crystallization of PVA in PAA/PVA blends is also completely suppressed when the PAA content is 38 mol% (or 50 wt%) [11]. The results can be taken to indicate that PVA interacts less strongly with PPMA as compared to PMTMA and PAA.

3.2. FTIR characterization

Fig. 2 shows the IR spectra in the 3000–3800 cm^{-1} region (O–H stretching) of PVA and various PPMA/PVA blends. The hydroxyl band of pure PVA consists of a broad band centered at 3483 cm^{-1} , attributed to a wide distribution of hydrogen-bonded hydroxyl groups. The center of the broad hydroxyl band of the blend shifts to a lower frequency (3438 cm^{-1}), showing the existence of the intermolecular hydrogen-bonding interactions between PVA and PPMA. In comparison, the hydroxyl band of PVA in PMTMA/PVA blends shows a larger low-frequency shift (from 3483 to 3427 cm^{-1}), indicating that the interaction in the PMTMA/PVA blends is stronger than that in PPMA/PVA blends. Fig. 3 shows the IR spectrum of carbonyl group of PPMA in 140 °C. PPMA has a strong carbonyl stretching absorption band at 1631 cm^{-1} . It is noted that the carbonyl band shows a slight low-frequency shift, indicating the involvement of carbonyl groups in interaction with PVA. In contrast, there is no significant

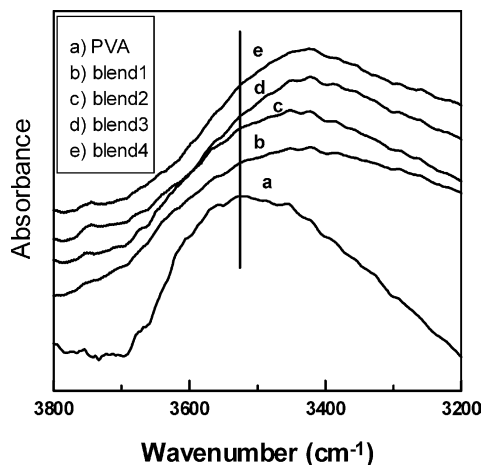


Fig. 2. FTIR spectra, recorded at 140 °C, of the hydroxyl stretching region of PPMA/PVA blends. (a) PVA; (b) PVA/PPMA (90/10); (c) PVA/PPMA (70/30); (d) PVA/PPMA (50/50); (e) PVA/PPMA (30/70).

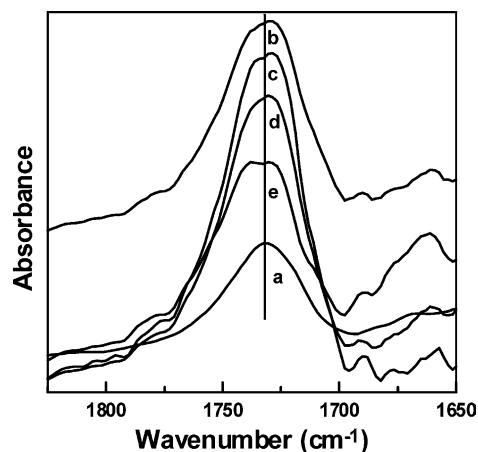


Fig. 3. FTIR spectra, recorded at 140 °C, of the carbonyl-stretching region of PPMA/PVA blends. (a) PPMA; (b) PVA/PPMA (90/10); (c) PVA/PPMA (70/30); (d) PVA/PPMA (50/50); (e) PVA/PPMA (30/70).

shift of the carbonyl band in PMTMA/PVA blends. The frequency shift of the carbonyl band in the PPMA/PVA blends is of the same magnitude as that observed in miscible poly(ϵ -caprolactone)/poly(vinyl chloride) blends [24,25]. The small frequency shift indicates a rather weak hydrogen bonding interaction. On the other hand, a stronger hydrogen bonding interaction, as in the case of miscible PPMA/PVPh blends [26], leads to the development of a new carbonyl band near 1700 cm^{-1} .

3.3. NMR characterization

Fig. 4 shows the ^{13}C CP/MAS spectra of PVA, PPMA and their blends, from which useful information can be drawn. Firstly, the methine carbon resonance of PVA is split into three peaks in its ^{13}C CP/MAS spectrum. The three peaks are designated as peaks 1, 2 and 3 in the order of decreasing frequency. The intensity of peak 2 is the strongest; hence the PVA used in this study is slightly

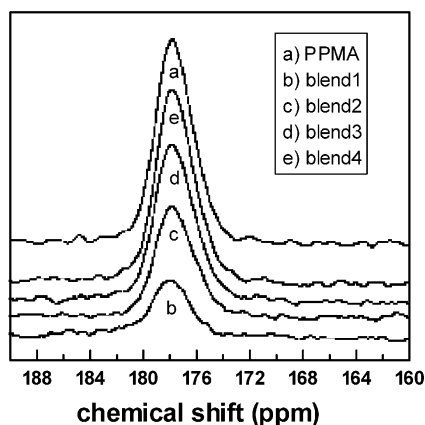
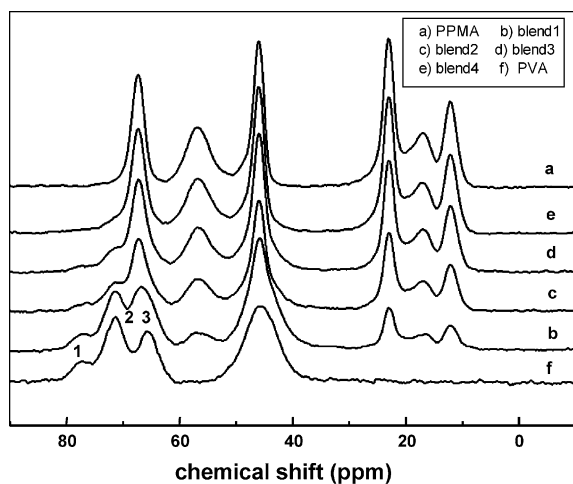


Fig. 4. ^{13}C CP/MAS spectra of PPMA, PVA, and their blends. (a) PPMA, (b) PVA/PPMA (90/10); (c) PVA/PPMA (70/30); (d) PVA/PPMA (50/50); (e) PVA/PPMA (30/70).

heterotactic [27]. According to Terao et al., the splitting of the methine carbon resonance reflects the stereo-regularity of PVA [27]. They assigned peak 1 to mm triad with two intramolecular hydrogen bonds, peak 2 to mm and mr triads with one hydrogen bond, and peak 3 to mm, mr, and rr triads with no intramolecular hydrogen bond. As shown in Fig. 4, peaks 1 and 2 of methine carbons of PVA are weakened with increasing PPMA content in the PPMA/PVA blends, but the three peaks of PVA can still be seen when the PPMA content is 75 wt%. For the PMTMA/PVA blends [17], when the PMTMA content is more than 72 wt%, the three peaks of methine carbon of PVA become very poorly resolved, almost merging into one broad peak. Therefore, from the changes of the three methine carbon peaks, it may be concluded that the addition of PPMA into PVA does not disrupt the formation of intramolecular and intermolecular hydrogen bonds of PVA as severely as that of PMTMA. The carbonyl carbon resonance peak of PPMA at 177.3 ppm shows a low-field shift of 0.5 ppm upon blending, indicating the involvement of carbonyl group of PPMA in interaction with PVA.

The scale of mixing in polymer blends can be determined through measurements of proton spin–lattice relaxation time in the rotating frame, $T_{1\rho}(H)$, and in the laboratory frame, $T_1(H)$. If the two polymer chains in a blend mix intimately, spin-diffusion occurs quickly among the chemically different components, which equilibrates the magnetization, and so single $T_{1\rho}(H)$ and $T_1(H)$ values are obtained. If not, different $T_{1\rho}(H)$ and $T_1(H)$ values are obtained for the carbons corresponding to different polymers. A single $T_1(H)$ value indicates mixing to a scale of about 20–30 nm, whereas a single $T_{1\rho}(H)$ value indicates mixing on a scale of about 1–3 nm [4,5,11]. The $T_{1\rho}(H)$ values are determined through delayed-contact ^{13}C CP/MAS experiments, using Eq. (1):

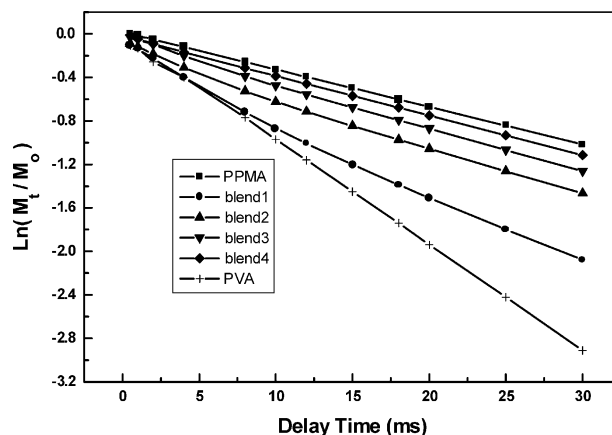


Fig. 5. Logarithmic plot of resonance of relative ^{13}C resonance intensity vs. delay time in PPMA/PVA blends. Blend 1: PVA/PPMA (90/10); blend 2: PVA/PPMA (70/30); blend 3: PVA/PPMA (50/50); blend 4: PVA/PPMA (30/70).

Table 2
 $T_{1\rho}(H)$ values of PPMA, PVA and PPMA/PVA blends

Resonance line (ppm)	$T_{1\rho}(H)$ (ms)					
	PPMA	10/90 ^a	30/70 ^a	50/50 ^a	70/30 ^a	PVA
23.5	28.9	18.5(35%) 4.1 (65%)	24.4(43%) 2.9 (57%)	25.6(46%) 2.1(54%)	27.5(47%) 1.2(53%)	
45						4.5(53%) 11.2(47%)
177.3	28.7	18.8(35%) 4.7 (65%)	24.8(43%) 3.2 (57%)	25.9(46%) 2.6(54%)	27.8(47%) 1.3(53%)	
70						4.3(54%) 11.0(46%)

^a Mole ratio of PPMA to PVA in the blend.

$$\ln \frac{M_\tau}{M_0} = \frac{-t}{T_{1\rho}(H)} \quad (1)$$

where τ is the spin-lock time used in the experiment, and M_0 and M_τ are the intensity of peak at zero time and at τ , respectively.

Fig. 5 shows the plots of $\ln(M_\tau/M_0)$ vs. τ , for the carbonyl carbon of PPMA and PVA/PPMA blends, and for the methylene carbon at 45 ppm for PVA. From the slope of the fitted line, the $T_{1\rho}(H)$ value was determined (Table 2). Pure PPMA shows a single-exponential decay with a $T_{1\rho}(H)$ value of 29 ms. On the other hand, PVA shows a bi-exponential decay and two $T_{1\rho}(H)$ values exist. The slow decay component (11.2 ms) would be attributed to crystalline phase, and the fast decay component (4.5 ms) to an intermediate phase [10,28]. Two $T_{1\rho}(H)$ values for various PPMA/PVA blends based on the carbon resonance peaks of PPMA exist. One is around 27 ms, which is attributed to PPMA-rich phase; the other is around 2–4 ms, which is attributed to miscible PPMA/PVA interphase. Therefore, the existence of two $T_{1\rho}(H)$ values for each blend based on PPMA carbon resonance peaks shows that the two polymers do not mix intimately to a scale of 1–3 nm, where the spin-diffusion occurs within the $T_{1\rho}(H)$ time.

To examine miscibility on a somewhat larger scale, the $T_1(H)$ values of various PVA/PPMA blends were measured and the results are summarized in Table 3. Only one composition-dependent $T_1(H)$ value for each blend sample is obtained, the value of which is intermediate to those of PPMA and PVA. Therefore, the PPMA/PVA blends are homogeneous on a scale of 20–30 nm [10].

Table 3
 $T_1(H)$ values of PPMA, PVA and PPMA/PVA blends

Resonance line (ppm)	$T_1(H)$ (s)					
	PPMA	10/90 ^a	30/70 ^a	50/50 ^a	70/30 ^a	PVA
23.5	0.59	5.7	3.7	2.3	1.5	
45						7.5
177.3	0.57	5.6	3.5	2.4	1.5	
70						7.4

^a Mole ratio of PPMA to PVA in the blend.

3.4. Melting point depression

The Flory–Huggins interaction parameter (χ_{12}) can be determined from the melting point depression data using the Nishi–Wang equation [29]:

$$\frac{1}{T_m} - \frac{1}{T_m^0} = -\frac{RV_{2u}}{\Delta H_{2u}V_{1u}}\chi_{12}(1 - \phi_2)^2 \quad (2)$$

where V_u is the molar volume of the repeating unit; ΔH_{2u} is the enthalpy of fusion of 100% crystalline polymer per mole of repeating unit; T_m^0 is the melting point of the pure crystallizable component; ϕ is the volume fraction. Eq. (2) is often written in the form

$$\Delta T_m = T_m^0 - T_m = -T_m^0 \left(\frac{V_{2u}}{\Delta H_{2u}} \right) B \phi_1^2 \quad (3)$$

where B , the interaction energy density, is related to χ_{12} by:

$$B = RT_m \left(\frac{\chi_{12}}{V_{1u}} \right) \quad (4)$$

The melting point results are plotted according to Eq. (3) as shown in Fig. 6. The slope of the line calculated by linear regression gives a value of -1.55 cal/cm^3 for B (using $V_{1u} = 117.01 \text{ cm}^3/\text{mol}$ and $T_m^0 = 225 \text{ }^\circ\text{C}$). The ΔH_{2u} and V_{2u} values of 100% crystalline PVA, respectively, are 1.6 kcal/mol and $32.7 \text{ cm}^3/\text{mol}$. The χ_{12} value is -0.31 which is less negative than that of the PAA/PVA blends (-1.24) [11]. The χ_{12} and B values were determined from the melting points obtained from a heating rate of $20 \text{ }^\circ\text{C/min}$ instead of the equilibrium melting points obtained from the Hoffman–Weeks extrapolation method. In their study on the

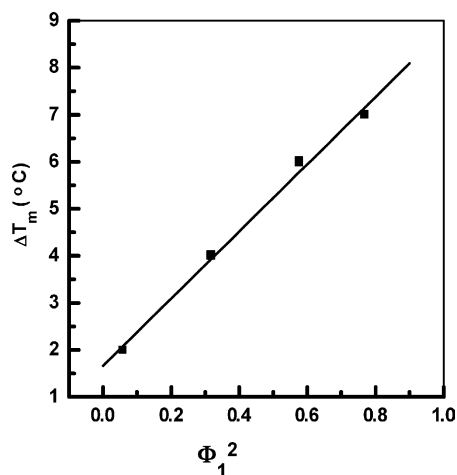


Fig. 6. Melting point depression plot of PPMA/PVA blends.

melting point depression of the PAA/PVA blends, Danilinc et al. [11] reported that successive thermal treatments induced crosslinking. The crosslinking modified crystallization parameters and introduced more errors than using the experimental melting points based on a fixed heating rate of 20 °C/min. Nevertheless, the small negative χ_{12} value for the PPMA/PVA blends suggests a weak interaction between the component polymers.

4. Conclusions

PPMA/PVA blends are miscible over the whole composition range based on the single- T_g criterion. Upon blending with PPMA, the hydroxyl band of PVA shifts to a low frequency. The frequency shift shows that the hydroxyl groups of PVA are interacting with PPMA. Interactions involving the carbonyl groups of PPMA are indicated by changes in the carbonyl absorption band and the ^{13}C carbonyl resonance peak. The $T_{1\rho}(H)$ and $T_1(H)$ results show that the blends are homogeneous on a scale of 20–

30 nm but not of 1–3 nm. The present study supports our previous suggestion that the big thioether sulfur atoms in the pendant groups of PMTMA reduce the accessibility of the carbonyl groups.

References

- [1] Coleman MM, Painter PC. *Prog Polym Sci* 1995;20:1.
- [2] Ping ZH, Nguyen QT, Neel J. *Makromol Chem* 1989;190:437.
- [3] Ping ZH, Nguyen QT, Neel J. *Makromol Chem* 1990;91:185.
- [4] Zhang X, Takegoshi K, Hikichi K. *Polymer* 1992;33:712.
- [5] Feng H, Feng Z, Shen L. *Polymer* 1993;34:2516.
- [6] Cassu SN, Felisberti MI. *Polymer* 1999;40:4845.
- [7] Parada LG, Cesteros LC, Meaurio E, Katime I. *Polymer* 1998;39:1019.
- [8] Aoi K, Takasu A, Okada M. *Macromol Rapid Commun* 1995;16:757.
- [9] Parada LG, Cesteros LC, Meaurio E, Katime I. *Macromol Chem Phys* 1997;198:2505.
- [10] Zhang X, Takegoshi K, Hikichi K. *Polym J* 1991;23:87.
- [11] Danilinc L, de Kesel C, David C. *Eur Polym J* 1992;28:1365.
- [12] Nishio Y, Manley RSJ. *Macromolecules* 1988;21:1270.
- [13] Cho YW, Nam CW, Jang J, Ko SW. *J Macromol Sci, Phys B* 2001;40:93.
- [14] Shuai X, He Y, Asakawa N, Inoue Y. *J Appl Polym Sci* 2001;81:762.
- [15] Park JW, Im SS. *Polymer* 2003;44:4341.
- [16] Yi JZ, Goh SH, Wee ATS. *Macromolecules* 2001;34:7411.
- [17] Yi JZ, Goh SH. *Polymer* 2003;44:1973.
- [18] Kwei TK. *J Polym Sci, Polym Lett Ed* 1984;22:307.
- [19] Pennachia JR, Pearce EM, Kwei TK, Bulkin BJ, Chen JP. *Macromolecules* 1986;19:1973.
- [20] Tubbs RK. *J Polym Sci A* 1965;3:4181.
- [21] Koyama N, Doi Y. *Polymer* 1997;38:1598.
- [22] Zhang L, Goh SH, Lee SY. *Polymer* 1998;39:4841.
- [23] Yoshie N, Azuma Y, Sakurai M, Inoue Y. *J Appl Polym Sci* 1995;56:17.
- [24] Varnell DF, Coleman MM. *Polymer* 1981;22:1324.
- [25] Coleman MM, Zarian DJ. *J Polym Sci, Polym Phys Ed* 1979;17:837.
- [26] Serman CJ, Painter PC, Coleman MM. *Polymer* 1991;32:1049.
- [27] Terao T, Maeda S, Saika A. *Macromolecules* 1983;16:1535.
- [28] Wang J, Cheung MK, Mi Y. *Polymer* 2001;42:3087.
- [29] Nishi T, Wang TT. *Macromolecules* 1975;8:909.